

Characteristics of the Ammonium Ion Adsorption from Wastewater by the Activated Carbon Obtained from Waste Tire

Ram Babu Ghising¹ and Vinay Kumar Jha²

¹Department of Nano Convergence Engineering, Jeonbuk National University, Jeonju, South Korea

²Central Department of Chemistry, Tribhuvan University, Kathmandu, Nepal

Corresponding Author's E-mail: vinayj2@yahoo.com

Submitted : 11 June 2022, Revised 22 June 2022, Accepted 23 June 2022

Abstract

The activated carbons were prepared from waste tire using a pyrolysis technique in different environments, namely: activated carbon in open air (AC-O), nitrogen gas (AC-N), nitrogen gas and water steam (AC-NW) and composite of tire and aluminum hydroxide in nitrogen and steam atmosphere (AC-COM), in order to study the change in specific surface area and making the composite of activated carbon and alumina. The X-ray diffraction study revealed the presence of quartz, alumina, zinc sulphide and activated carbon. Methylene blue adsorption isotherm showed that the highest specific surface area of 218m²/g was found in case of activated carbon prepared in oxygen atmosphere and subsequently used for ammonium ion adsorption. The adsorption isotherm, and kinetic behavior were studied with optimum pH 9. The adsorption isotherm fitted well to the Freundlich Model than that of Langmuir and equilibrium monolayer adsorption capacity calculated from Langmuir was 277.8 mg/g at room temperature. The adsorption reached equilibrium in 120 minutes, and kinetic data fitted well to the pseudo-second order model with rate constant value 5.3×10⁻³ L g/(mg·min). Real water samples from different places within Kathmandu valley were subjected for ammonium ion adsorption onto the active carbon and were worked for the adsorption smoothly.

Keywords: Activated carbon; Adsorption isotherm; Ammonium ions; Methylene blue; Waste tire

1. Introduction

The durability of tires which is desirable property make their disposal difficult due to biologically non-degradable and hence shows major environmental issue globally [1]. It is estimated that over 3.4 million tons of waste tires are generated in Europe, 4.6 million tons in the US and greater than 1 million tons in Japan per year [2].

Burning tires in roads and highways has been a popular custom to demonstrate any kind of protests. This results in the emission of large amounts of thick black smoke and noxious gases including carcinogens which is a major source of air pollution. On the other hand, scrap tires are ground and used in asphalt for

paving streets and highways, as a low weight, high volume fill for septic systems, play ground covers, drainage and fill materials for turf grasses, in molded goods, and more. Similarly, scrap tires are shredded and used as much in flower beds, as landfill liners and daily covers. Moreover, whole scrap tires are used in retaining walls, in embankments, as artificial reefs and break waters or they are baled whole and used in engineering and construction applications.

The various scrap tire pyrolysis processes, such as fluidized beds, a shaft furnace, an extruder and a rotary kiln, have been used. There is a relationship between pyrolysis temperature and the quality of the produced char [3]. It was found that the pyrolytic

char produced by pyrolysis in a steam atmosphere had a very clean surface, without tarry deposits, and possessed characteristics of the original carbon black that was used in tire production [4]. The chemical structure of the rubber tire with that of coal was compared and pyrolysis was carried out before an oxidation pretreatment [5]. It was found that high pressure oxygen pretreatment of tires would increase the oxygen functional group content which favors cross-linking reactions during pyrolysis, thereby increasing char yield. This approach may be important if char yield in a pyrolysis process is to be maximized. The scrap tire vacuum pyrolysis process developed by Roy at Laval University, Quebec, operates under sub-atmospheric pressures ranging from 0.30 to 20 kPa and temperatures ranging from 420 to 700 °C [6]. It was shown that both pyrolysis temperature and pressure have a major influence on the properties of the recovered char. Pyrolytic carbon black deposits decrease with lowering of pressure and increase with pyrolysis temperature. Studies have been carried out to investigate the use of pyrolytic char as a precursor for active carbon production [2, 6, 7]. The active carbon-alumina composites obtained from waste rubber tire and aluminumhydroxide by pyrolytic technique at 700 °C in nitrogen and steam environment were used to remove As(III) and As(V) from aqueous solution phase [8]. Similarly, hydrogen peroxide activated carbon synthesized from waste tire was used as removal of Cd(II) and Pb(II) from domestic wastewater [9].

Eventhough nitrogen containing compounds are necessary for living organisms, their high content exceeding the requirement can cause more eutrophication with in lakes and rivers, depletion in dissolved oxygen and toxicity in fish within water [10]. Thus, nitrogen pollution in hydrosphere has recently attracted increasing attention for eutrophication of lakes and rivers all over the world. Ammonium is the inorganic ion form of nitrogen pollution contained in municipal sewage, industrial wastewater and agricultural wastes or decomposed from organic nitrogen compounds in wastewater and wastes. Higher concentration of ammonium ion will cause a sharp decrease of dissolved oxygen

and obvious toxicity on aquatic organisms [11]. The traditional method for ammonium ion removal from municipal and industrial wastewater is based on biological treatments [12]. However, as the discharge limits of different pollutants are more stringent, ion exchange and adsorption are gaining momentum as available methods for the treatment of waters polluted with ammonium ions. The removal of ammonia and ammonical ions through biological methods i.e. nitrification is not getting more response due to the appearance of unacceptable peaks in effluent ammonium concentration and the variable concentration of it is more toxic to fish than constant concentration [13]. To adsorb nitrite, nitrate and ammonium ion from aqueous solutions, ion chromatography was employed in which active carbon prepared from commercially available carbon treated with hydrogen peroxide followed by hydrochloric acid and methanol was used as adsorbent material [14]. Similarly, ammonium ion from fish farms was also removed by active biochar obtained from rice straw [15].

A study of the adsorption of Mn onto the activated carbon obtained from tire residual showed the maximum adsorption capacity of 120 mg/g and the process of adsorption followed pseudo second order kinetics and Freundlich isotherm model [16].

The pyrolysis char derived from the waste vehicle tires and high density polyethylene showed the maximum Cr(VI) adsorption capacity of 14.09 mg/g and the process of adsorption followed pseudo first order kinetics and Temkin as well as Langmuir isotherm models [17].

Activated carbon is one of the most widely used materials for environmental applications like gas separation, deodorant use, solvent recovery and water purification because of its superior sorption ability corresponding to its high specific surface area [18]. There are very few studies regarding the adsorption of ammonium ion from water with the activated carbon obtained from waste tire. Hence, this paper deals with preparation of activated carbons from waste tire, their characterizations and application to the removal of ammonium ion present in real water system.

2. Materials and Methods

2.1 Preparation of adsorbents and reagents

2.1.1 Collection of waste tire and its pyrolysis

The waste tires were collected from resoling center, treated with 5M hydrochloric acid, washed and dried in sunlight. They were subjected to pyrolysis at 700 °C in different atmospheres to produce different active carbons such as active carbon in open air (AC-O), nitrogen gas (AC-N) and mixture of nitrogen gas and water steam (AC-NW). The activated carbon-alumina composite (AC-COM) was also produced by 50:50 proportions of tire pieces and aluminum hydroxide in nitrogen and steam atmosphere.

2.1.2 Reagent preparation

A methylene blue solution of 0.5g/L was prepared in 500 mL volumetric flask. An ammonium chloride of weight 1.485 g, dried at 100 °C for 1 hour, was weighed and made 500 mL standard solution with the help of de-ionized water. Likewise, 0.5% w/v sodium nitroprusside solution and 11.10% v/v alcoholic phenol solution were also prepared. Additionally, an alkaline citrate solution was made by dissolving 20 g tri-sodium citrate and 1.086 g sodium hydroxide pellets in 100 mL volumetric flask.

2.1.3 Determination of specific surface area

To determine the specific surface area of the activated carbons, the Langmuir adsorption isotherm model was used. A 25 mg activated carbon was weighed out accurately and transferred to 25 mL conical flasks containing 20-100 mg/L concentrations of methylene blue solutions. The solutions were then shaken for 4 continuous hours in a mechanical shaker. It was then allowed to rest for half an hour. Doing so the carbon settled down and the supernatant solution was pipetted out. The absorbance of the resultant solution was taken at 660 nm wavelength. From the Langmuir adsorption isotherm, maximum adsorption capacity, Q_m , was determined. And, the specific surface area of each type of activated carbon was determined using the following formula [19]:

$$S_{MB} = \frac{N_g \times a_{MB} \times N \times 10^{-20}}{M} \dots \dots \dots (i)$$

Where, S_{MB} is the specific surface area in $10^{-3} \text{ km}^2\text{kg}^{-1}$, N_g is the number of molecules of methylene blue adsorbed at the monolayer of activated carbon in kg/kg (or $N_g = N_m \times M$), a_{MB} is the occupied surface area of one molecule of methylene blue = 197.2 \AA^2 [20], N is Avogadro's number (6.023×10^{23}), M is the molecular weight of methylene blue (319.85 g mol) and $\frac{N_g}{M}$ gives mmol/g which is equivalent to the Q_m of the Langmuir equation.

2.2 Effect of pH

For the pH studies of ammonium ion adsorption, the initial concentration and volume of solution taken were 20 mg/L and 25 mL respectively. The solutions were taken in 50 mL conical flasks and the pH of the solutions was adjusted from 5 to 10 using appropriate strength of NaOH and HCl solutions with the help of pH meter (Model 270, Denver Instrument, Japan). To each flask, 25 mg AC-O activated carbon adsorbent was added and then shaken in shaker for 20-24 hours. After shaking, each solution was filtered immediately using Whatman 41 filter paper and the equilibrium pH of the filtrate was noted. The filtrates were analyzed using spectrophotometer at 630 nm to determine the equilibrium concentration of ammonium ion. With the help of initial concentration (C_i) and equilibrium concentration (C_e), the percentage adsorption of ammonium ion at each pH was determined by the following formula:

$$\text{Adsorption \%} = \frac{(C_i - C_e)}{C_i} \times 100\% \dots \dots \dots (ii)$$

2.3 Ammonium ion adsorption

2.3.1 Adsorption isotherms

The adsorption isotherm study was done with different initial concentrations of ammonium ion ranging from 50 to 600 ppm with 25 mg of AC-O activated carbon adsorbent. The solutions were shaken mechanically for 24 hours. The equilibrium concentrations of ammonium ion after adsorption were determined by Phenate Method using spectrophotometer [21]. Here, Langmuir [22], and Freundlich [23] models given by mathematical equations (iii) and (iv), respectively,

had been tested to study the adsorption isotherm behavior.

$$\frac{C_e}{Q_e} = \frac{1}{Q_m b} + \frac{C_e}{Q_m} \dots\dots\dots (iii)$$

$$Q_e = K_F C_e^{\frac{1}{n}} \dots\dots\dots (iv)$$

Where Q_e (mg/g) is the amount of adsorbate adsorbed per unit mass of adsorbent, C_e (mg/L) is the equilibrium concentration of the adsorbate, Q_m (mg/g) is the maximum adsorption capacity and ‘b’(L/mg) is the Langmuir adsorption equilibrium constant, K_F [(mg/g)(L/mg)^{1/n}] and n(g/L) are Freundlich equilibrium coefficients, which are considered to be the relative indicators of adsorption capacity and adsorption intensity

2.3.2 Kinetic behavior

To study kinetic behavior, 25 mL of 20 ppm ammonium ion solution in a 50 mL conical flask containing 25 mg AC-O activated carbon was used. The reaction mixture was shaken for different length of time, 10 to 200 minutes, in a mechanical shaker at constant speed. The kinetics of ammonium ion adsorption were investigated by taking out reaction mixture at the desired period of contact time and immediately filtered through filter paper to obtain filtrates. The concentrations in the filtrates were determined spectrophotometrically. The data obtained were tested with pseudo-first order [24] and pseudo-second order [25] kinetic models. The linearized forms of pseudo first and pseudo second order models are given by equations (v) and (vi).

$$\log(Q_e - Q_t) = \log Q_e - \frac{k_1}{2.303} t \dots\dots\dots (v)$$

Where, Q_e (mg/g) is the amount of adsorbate adsorbed at equilibrium and Q_t (mg/g) is the amount of adsorbate adsorbed at any time ‘t’. Similarly, k_1 (min⁻¹) is the rate constant of pseudo-first order adsorption.

$$\frac{t}{Q_t} = \frac{1}{k_2 Q_e^2} + \frac{1}{Q_e} t \dots\dots\dots (vi)$$

Where k_2 (L g/mg min) is the pseudo-second order rate constant and Q_e and Q_t are the amount of adsorbate adsorbed at equilibrium and any time ‘t’ respectively.

2.4. Characterization of adsorbents

2.4.1 Fourier transform infrared (FTIR)

The functional groups of activated carbon AC-O before and after ammonium ion adsorption were identified using FT-IR Spectrophotometer (IRPrestige-21, Shimadzu, Japan). The fine powder sample with KBr pellets was prepared in the size range of about 10-13 mm in diameter and 1 mm in thickness. The samples were then scanned in the spectral range of 400 – 4500 cm⁻¹.

2.4.2 X-ray diffraction (XRD)

All the four samples prepared in different environments, without any adsorption, were analyzed for the elemental detection using X-ray Diffractometer with monochromatic Cu Kα radiation (D2 Phaser Diffractometer, Bruker, Germany) at Nepal Academy of Science and Technology (NAST). The samples were scanned at 2θ from 10 to 80°.

2.5 Adsorption on ground water

Underground water samples were collected from four different places and analyzed for ammonium ion content in them. The study was also carried out to investigate the ammonium ion content after adsorption in the real water system by taking 25 mL water samples in 50 mL conical flasks. To each flask, 25 mg AC-O activated carbon was added after maintaining optimum pH and then shaken in a mechanical shaker for 24 hours. The solutions were then filtered and the filtrates thus obtained were analyzed for remaining ammonium ion content.

3. Results and Discussion

3.1 Analysis of active carbons

3.1.1 XRD study

The phase properties (amorphous or crystalline type) of activated carbons are fundamental parameters for the contaminant adsorption effectiveness. It has been shown for activated carbon that high specific surface area contributes to high adsorption capacity and favorable pore structure facilitates fast mass transfer

or intra-particle diffusion. The XRD patterns of all the four type activated carbons are shown in Fig.1.

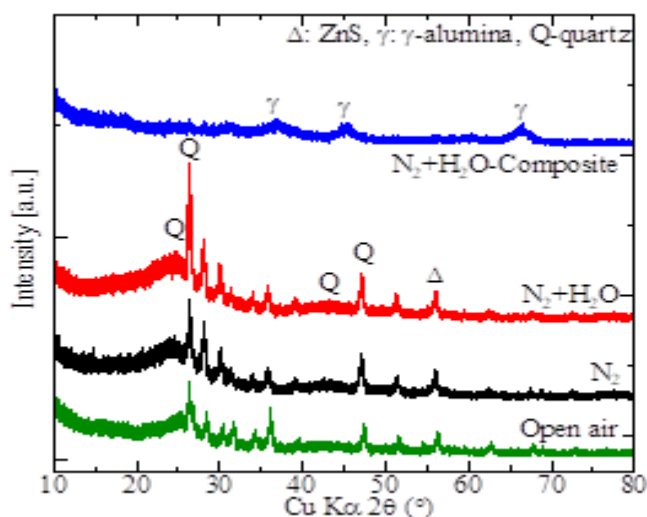


Fig. 1: XRD pattern of all four types of different activated carbons before any adsorption.

Some sharp XRD peaks observed at $2\theta = 24.7^\circ$, 26.61° , and 47.20° were attributed to quartz. that at 37 , 46.50° and 66.60° as γ -alumina (JCPDS Card No. 00-010-0425). The peak appeared at 56.50° was due to ZnS of (311) plane [26]. The broad humps in the regions $24-26^\circ$ and $42-45^\circ$ [27] were due to the presence of amorphous activated carbon. Rubbers in tire are cross-linked through sulphur (acts as an accelerator) and an activator (which usually consists of zinc oxide and stearic acid) [28]. The presence of ZnS in XRD pattern of waste tire derived adsorbents is due to the presence of sulfur and zinc. Some minerals are normally used as filler agents in the process of tire manufacturing and hence not all peaks were analyzed.

3.1.2 Comparative study of specific surface area of activated carbons

To determine the specific surface area, the linearized Langmuir curve was drawn. The curves of four different types of activated carbons are shown in Fig. 2 and the corresponding Langmuir parameters are shown in Table 1. The specific surface areas of the activated carbon were calculated with the help of slopes obtained from the curves. The specific surface areas of the AC-O, AC-N, AC-NW and AC-COM were found 218, 120, 112 and $77 \text{ m}^2/\text{g}$, respectively.

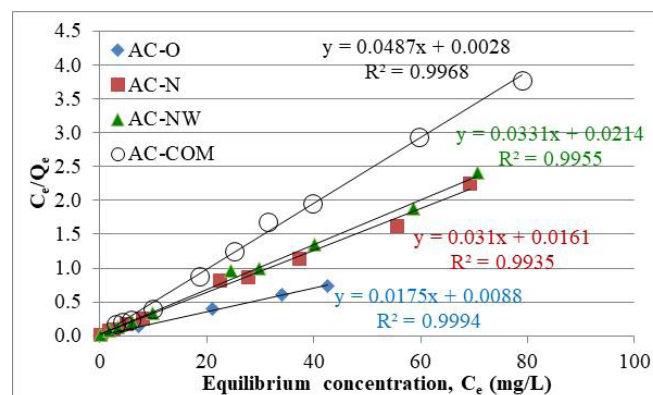


Fig. 2: A plot of C_e/Q_e versus C_e of active carbons.

Table 1: Langmuir parameters for adsorption of methylene blue

Adsorbent	Langmuir parameters		R ²
	Q _m (mg/g)	b(L/mg)	
AC-O	57.14	1.99	0.9968
AC-N	32.26	1.93	0.9935
AC-NW	30.21	1.55	0.9955
AC-COM	20.53	17.40	0.9968

On comparison of AC-O, AC-N and AC-NW, the AC-O has the highest specific surface area and that of AC-NW has the lowest. The maximum specific surface area of AC-O is due to high ash content. During $\text{N}_2+\text{H}_2\text{O}$ activation in case of AC-NW, low ash content is formed on the surface due to removal of ash by the flow of nitrogen gas [29]. The lower specific surface area of activated carbon AC-NW may also be attributed to other impurities which block the pores of the activated carbons [30]. Since the AC-COM was obtained by pyrolysis of 50:50 proportions of aluminum hydroxide and tire pieces, the lower specific surface area was to be expected. The activated carbon prepared from rice husks after 10% ZnCl_2 impregnation was found to have highest surface area as $480 \text{ m}^2/\text{g}$ and the concentration below and above had lower area [31] but in the case of waste tire which already contains Zn as an activator ZnCl_2 may not work as an efficient activator further. Due to the highest specific surface area of Ac-O sample among the four types of adsorbent materials prepared from waste tire, this adsorbent (Ac-O) was selected for further adsorption studies.

3.1.3 Fourier Transform Infrared Analysis

The distinct peak of ammonium ion can't be observed, however the spectra of AC-O before and after ammonium ion adsorption are shown in **Fig. 3**. The AC-O has intense peak ranging from 2850-3000 cm^{-1} due to the C-H stretching. The distinct and intense peak at 3490 cm^{-1} is indicative of overlapped O-H and N-H stretching groups [32]. The peak at 1613 cm^{-1} could be attributed to N-H bending. Peaks appearing at 671 cm^{-1} , 520 cm^{-1} , 460 cm^{-1} are assigned as of Si-O symmetrical bending, Al-O-Si deformation as well as Si-O stretching and O-Si-O/O-Al-O bending vibrations respectively [33]. Concluding it can be easily noticed that there are no differences, not to the peaks nor to the shifting before and after ammonium adsorption indicating that NH_4^+ adsorption did not alter the structure of AC-O. However, the intensity of the broad combined peaks in the range of 1736-1590 cm^{-1} is expected to be due to the adsorption of NH_4^+ on activated carbon obtained from waste tire [34].

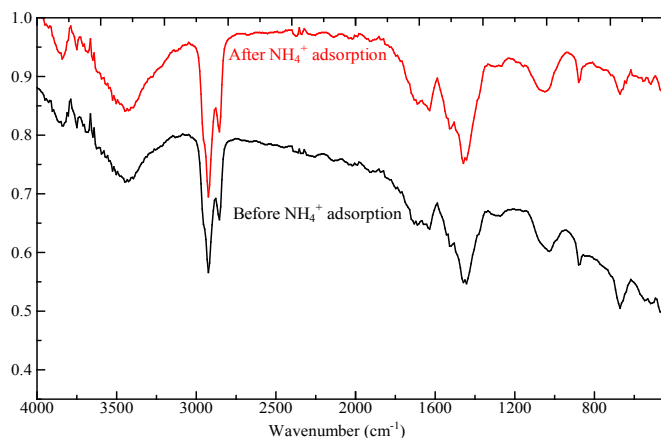


Fig. 3: FTIR spectra of AC-O before and after ammonium ion adsorption

3.2 Optimum pH

The effect of pH on adsorption process is illustrated in **Fig. 4** which shows the relationship between percentage of adsorption and the initial pH in the adsorption of NH_4^+ ion onto AC-O at an initial concentration of 20 ppm (mg/L). In this study, the NH_4^+ ion was adsorbed by varying the pH from 5 to 10. The maximum adsorption percentage was found at pH 9, which was 40.45%. Hence the pH 9 was designed as optimum pH. It was found that the ammonium ion adsorption increased with increasing pH and the maximum adsorption value at pH 9 and

then declined with further increase. A similar trend was observed for the adsorption of ammonium ion by coconut shell-activated carbon and by zeolites synthesized from fly ash [35]. This may be explained that the lower ammonium ion adsorption is due to the competition of H^+ and NH_4^+ ions for the exchange of sites on adsorbent surfaces. This translated that the adsorption of ammonium ion onto AC-O decreased with a decrease in solution pH. This ionic competitiveness may disappear when the aqueous solution pH increase [36]. At alkaline pH, the active sites of the adsorbent become negatively charged, which enhanced the binding of ammonium ion onto adsorbent. Beyond pH 9 the NH_4^+ ions get converted to NH_3 and hence decrease in the adsorption. Similar trend was observed for ammonium ion adsorption by bio-adsorbent - cotton waste and Boston ivy leaf powder [37].

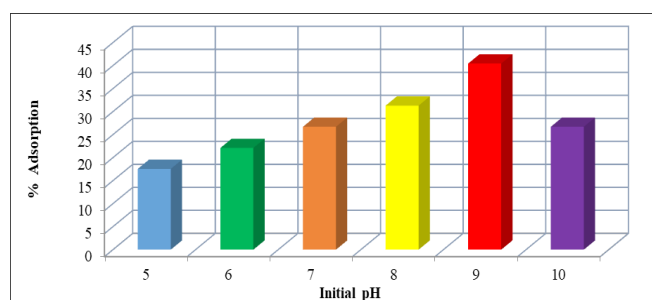


Fig.4: A plot of Adsorption (%) versus initial pH of the ammonium ion solution.

3.3 Ammonium adsorption isotherm study

The Langmuir and Freundlich models were used to fit the experimental data which are shown in the **Fig. 5 (a) and (b)**.

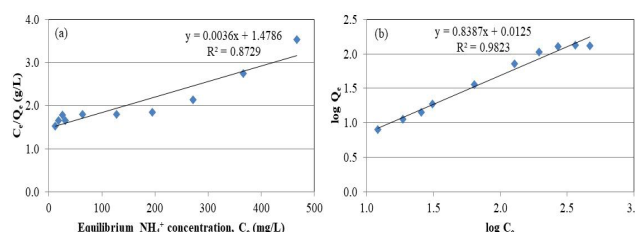


Fig.5: The linearized (a) Langmuir and (b) Freundlich curves for the adsorption of ammonium ion onto AC-O.

The ammonium adsorption capacity of AC-O increased with the increase of initial ammonium concentration and then attained the upper limit which is shown in the **Fig. 6**.

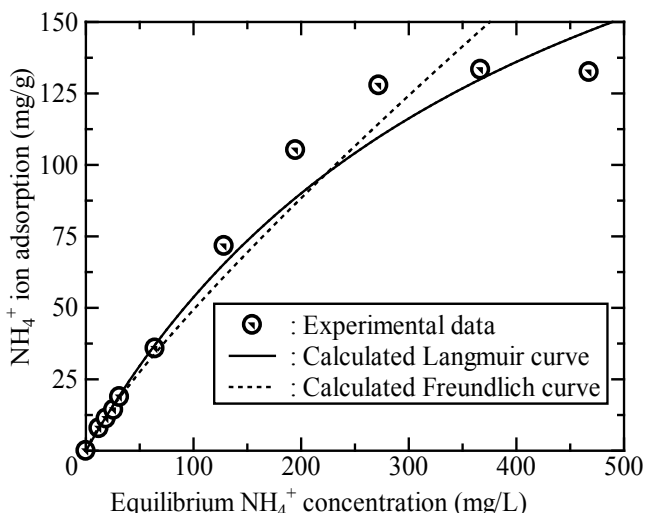


Fig.6: The adsorption isotherm of ammonium ion onto AC-O

The increase in adsorption was due to the high probability of collision between the ammonium ions and adsorbent surface. The attainment of the upper limit was attributed to the availability of limited active sites. Similarly, Table 2 shows the parameters of Langmuir and Freundlich isotherms. Since the coefficient of determination (R^2) of Freundlich model is greater than that of the Langmuir, so the adsorption of ammonium ion onto AC-O was stacked adsorption with heterogeneous surfaces.

Table 2: Parameters of Langmuir and Freundlich Models

Langmuir Model		R^2	Freundlich Model	
Q_m (mg/g)	b (L/mg)		K_f [(mg/g) (L/mg) ^{1/n}]	n
277.8	0.0024	0.8729	1.03	1.19

This implies that the experimental data fitted well to the Freundlich model which matched with previous reports [37, 38]. The maximum adsorption capacity of waste-tire based activated carbon was found to be 277.8 mg/g, which is significantly higher than the ones obtained from the bio-adsorbents and mineral adsorbents. The Q_m values obtained for Boston ivy leaf powder, synthesized zeolites NaY and natural zeolites (Dogantepe) are 6.59, 42.37 and 25.77 mg/g respectively [37, 39, 40]. The ammonium ion adsorption capacity of biochar obtained from rice straw for the removal of ammonium from fish farms was found to be 4.251 mg/g [15]. Similarly, the adsorption capacity of commercially available carbon followed

by activation with hydrogen peroxide, hydrochloric acid and methanol was 0.0128 mg/g [14].

3.4 Kinetic Studies

The study of adsorption kinetics describes the solute uptake and the time required for the adsorbate uptake at the solid-solution interface. For kinetic studies, the effect of contact time and two models: pseudo-first order and pseudo-second orders, were employed to the experimental kinetic data as shown in Figs. 7 and 8.

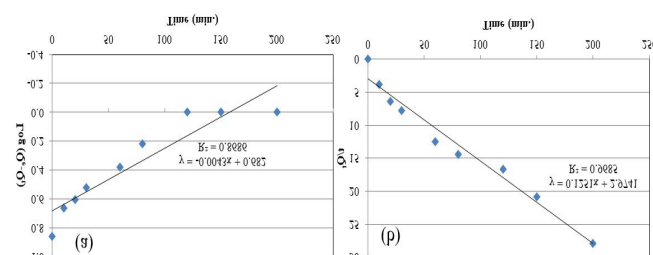


Fig.7: (a) Pseudo-first order and (b) Pseudo-second order kinetic models for the adsorption of ammonium ion onto AC-O.

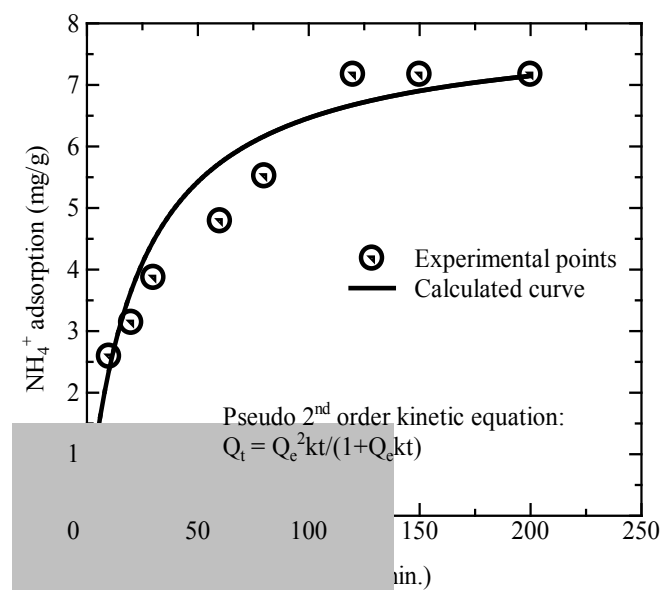


Fig. 8: Effect of contact time on adsorption of ammonium ion onto AC-O.

Table 3: Kinetic data for the adsorption of ammonium ion onto AC-O.

Reaction order	Rate constant K_1 (min ⁻¹)	Q_e value K_2 (Lg/mg min)	R^2
Pseudo-first	0.00991.98	0.8686	
Pseudo-second	0.00537.98	0.9685	

It is very clear from the graph that the equilibrium reached in 120 minutes. The same result was obtained in the previous reports [38]. It was found that the adsorption rate was rapid at first and then slowed down near the equilibrium state. After reaching the saturation point there was no significant change in the rate. The initial rapid increase in the rate was due to the availability of more number of active sites so that large number of ammonium ions got attached to adsorbent sites. As the time passed the number of active sites became less and finally the equilibrium state was achieved. The correlation coefficient values of pseudo-first order and pseudo-second order models were determined as 0.8686 and 0.9685 respectively showing that the kinetics of ammonium ion onto AC-O followed pseudo-second order with rate constant value 5.3×10^{-3} L g/(mg min) as shown in Table 3.

3.5. Underground water sample analysis

The waste water collected from different places of Kathmandu valley were analyzed for ammonium ion content by the Phenate Method which is shown in Table 4.

Table 4: Analysis of ammonium ion adsorption of water samples from different places

Places	Initial Concen. (mg/L)	Equil. Concen. (mg/L)	Difference	Adsorption (%)
Kirtipur	31.16	22.45	8.71	27.94
Lokanthali	13.74	10.74	3.02	21.97
Bhaktapur	16.30	12.64	3.66	22.45
Balaju	08.25	6.78	1.47	17.80

From Table 4, it is clear that Kirtipur has highest content of ammonium ion 31.16 mg/L and that of Balaju has 8.25 mg/L. The WHO standard value of ammonium ion in potable water is 0.41 mg/L. All the water samples collected were subjected for the adsorption by AC-O. All the ammonium ion content

was not adsorbed from any sample due to the presence of appreciable calcium ion, magnesium ion, hydrogen sulfide and other interfering ions may be present in the water sample but which were not analyzed due to some limitations in the work place.

4. Conclusions

Three types of activated carbons along with a composite of activated carbon and alumina were obtained from waste tire. The activated carbon AC-O was used for ammonium ion adsorption as specific surface area of this type of activated carbon was found the highest (218 m²/g) among the four types of adsorbent materials. The optimum pH for ammonium ion adsorption was obtained as 9. The adsorption isotherm study revealed that the Freundlich model fitted better than that of the Langmuir model. The equilibrium contact time was found 120 minutes following the pseudo-second order kinetic model with rate constant value 5.3×10^{-3} L g/(mg min). Moreover, activated carbon AC-O was also utilized to remove the ammonium ion present in wastewater and results showed that all ammonium ions content adsorption was not achieved which was due to the presence of appreciable amounts of interfering ions in the water system.

Acknowledgements

RB Ghising is thankful for M.Sc. Thesis Support and VK Jha is thankful for Faculty Research Grant to University Grants Commission (UGC), Bhaktapur, Nepal (FR-068/069-18, 2012). We are grateful to Dr. Suresh Kumar Dhungel of Nepal Academy of Science and Technology (NAST) for his valuable help in X-Ray diffraction measurement of samples. We would like to acknowledge Mr. Keshav Paudel, Department of Plant Resources, Thapatali, for providing FT-IR data.

References

- [1] E. L. K. Mui, D. C. K. Ko and G. McKay, Production of active carbons from waste tyres- a review, *Carbon*, 2004, 42 (14), 2789-2805. (DOI: <https://doi.org/10.1016/j.carbon.2004.06.023>)
- [2] I. F. Elbaba, and P. T Williams, Two stage pyrolysis-catalytic gasification of waste tyres: Influence of process parameters, *Applied Catalysis B: Environmental*, 2012, 125, 136-143. (DOI: <https://doi.org/10.1016/j.apcatb.2012.05.020>)
- [3] S. Kawakami, K. Inoue, H. Tanaka and T. Sakai, Thermal conversion of solid wastes and biomass (Edited by J. L. Jones and S. B. Radding), *American Chemical Society Symposium Series*, 1980, 130, 557-572. (DOI: 10.1021/bk-1980-0130)
- [4] G. Crane, R. A. Elefritz, E. L. Kay and J. R. Laman, Scrap tire disposal procedures, *Rubber Chemistry and Technology*, 1978, 51 (3), 577-599. (DOI: <https://doi.org/10.5254/1.3535750>)
- [5] H. Teng, M. A. Serio, R. Bassilakis, P. W. Morrison and P. R. Solomon, *American Chemical Society, Division of Fuel Chemistry*, 1992, 37, 533-554.
- [6] C. Roy, A. Rastegar, S. Kaligauine, H. Darmstadt and V. Tochev, Physicochemical properties of carbon blacks from vacuum pyrolysis of used tires. *Plastics, Rubber Composites, Processes and Their Applications*, 1995, 23, 21-30. (<https://www.infona.pl/resource/bwmeta1.element.elsevier-4d93b84e-bc6d-361e-8a13-45a901577bc1>)
- [7] P. T. Williams, S. Besler, D. T. Taylor, The pyrolysis of scrap automotive tires: The influence of temperature and heating rate on product composition, *Fuel*, 1990, 69 (12), 1474-1482. (DOI: [https://doi.org/10.1016/0016-2361\(90\)90193-T](https://doi.org/10.1016/0016-2361(90)90193-T))
- [8] M. S. Karmacharya, V. K. Gupta, I. Tyagi, S. Agarwal and V. K. Jha, Removal of As(III) and As(V) using rubber tire derived activated carbon modified with alumina composite. *Journal of Molecular Liquids*, 2016, 216, 836-844. (DOI: <http://dx.doi.org/10.1016/j.molliq.2016.02.025>)
- [9] K. M. Dimpe, J. C. Ngila and P. N. Nomngongo. 2017. Application of waste tire-based activated carbon for the removal of heavy metals in wastewater, *Journal Cogent Engineering*, 2017, 4 (1), 1-11. (DOI: <https://doi.org/10.1080/23311916.2017.1330912>)
- [10] V. K. Jha and S. Hayashi, Modification on natural clinoptilolite zeolite for its ammonium ion retention capacity, *Journal of Hazardous Materials*, 2009, 169(1), 29-35. (doi:10.1016/j.jhazmat.2009.03.052)
- [11] X. C. Zeng and Y. X. Li. 1998. Technology of phosphorous and nitrogen removal from wastewater. China Architecture and Building Industry Press, Beijing.
- [12] G. Kiely G. 1996. *Environmental Engineering*, Mc-Grawl Hill Publishing Company, Maidenhead, England, 1996.
- [13] T. C. Jorgenson and L. R. Weatherly, Ammonia removal from wastewaters by ion-exchange in the presence of organic contaminants, *Water Resources*, 2003, 37, 1723-1728. (DOI: 10.1016/S0043-1354(02)00571-7)
- [14] A. Gierak and I. Lazarska, Adsorption of nitrate, nitrite and ammonium ions on carbon adsorbents, *Adsorption Science and Technology*, 2017, 35(7), 721-727. (<https://doi.org/10.1177/0263617417708085>)
- [15] A. Khalil, N. Sergeevich and V. Borisova, Removal of ammonium from fish farms by biochar obtained from rice straw: Isotherm and kinetic studies for ammonium adsorption, *Adsorption Science and Technology*, 2018, 36(5), 1294-1309. (<https://doi.org/10.1177/0263617418768944>)
- [16] M. Niksirat, R. Sadeghi, and J. Esmaili, Removal of Mn from aqueous solutions, by activated carbon obtained from tire residuals, *SN Applied Sciences*, 2019, 1, 782-793. (DOI: <https://doi.org/10.1007/s42452-019-0797-5>)

- [17] M. Kalem, E. Yel and Z. Arıkan, The adsorption of Cr(VI) and organic matter by new generation pyrolysis char, Dicle University Journal of Engineering, 2021, 12(2), 285-296. (DOI: 10.24012/dumf.773523)
- [18] K. Okada, V. K. Jha, Y. Kameshima, A. Nakajima and K. L. D. MacKenzie. Sorption properties of activated carbon derived from used paper and of amorphous $2\text{CaO}\cdot\text{Al}_2\text{O}_3\cdot 2\text{SiO}_2$ from paper sludge ash, Waste Management in Japan 2004, 79, 51-60. (DOI: 10.2495/WMJ040061)
- [19] A. U. Itodo, H. U. Itodo and M. K. Gafar, Estimation of specific surface area using Langmuir isotherm method, Journal of Applied Sciences and Environmental Management, 2010, 14(4), 141-145. (DOI: 10.4314/jasem.v14i4.63287)
- [20] C. Kaewprasit, E. Hequet, N. Abidi, and J. P. Gourlot. Application of Methylene Blue Adsorption to Cotton Fiber Specific Surface Area Measurement: Part I. Methodology, The Journal of Cotton Science, 1998, 2, 164-173. (<https://www.cotton.org/journal/1998-02/4/upload/jcs02-164.pdf>)
- [21] C. N. Sawyer, P. L. McCarty and G. F. Parkin, 1994. Chemistry for Environmental Engineering, Illustrated edition, McGraw - Hill, Inc. 2003.
- [22] I. Langmuir, The adsorption of gases on plane surfaces of glass, mica and platinum, Journal of American Chemical Society, 1918, 40(9), 1361-1403. (DOI: <https://doi.org/10.1021/ja02242a004>)
- [23] H. Freundlich and W. Heller, The adsorption of *cis*- and *trans*-Azobenzene, Journal of American Chemical Society, 1939, 61(8), 2228-2230. (DOI: <https://doi.org/10.1021/ja01877a071>)
- [24] S. Lagergren, Zur theorie der sogenannten adsorption gelöster stoffe. Kungliga svenska vetenskapsakademiens. Handlingar, 1898, 24, 1-39
- [25] Y. S. Ho and G. McKay, Pseudo-second order model for sorption processes, Process Biochemistry, 1999, 34(5), 451-465. (DOI: [https://doi.org/10.1016/S0032-9592\(98\)00112-5](https://doi.org/10.1016/S0032-9592(98)00112-5))
- [26] C. S. Pathak, M. K. Mandal and V. Agarwala, Synthesis and characterization of zinc sulphide nanoparticles prepared by mechanochemical route, Superlattices and Microstructures, 2013, 58, 135-143. (DOI: <https://doi.org/10.1016/j.spmi.2013.03.011>)
- [27] M. S. Karmacharya, V. K. Gupta and V. K. Jha, Preparation of activated carbon from waste tire rubber for the active removal of Cr(VI) and Mn(II) ions from aqueous solution, Transactions of the Indian Ceramic Society, 2016, 75, 234-241. (DOI: <https://doi.org/10.1080/0371750X.2016.1228481>)
- [28] C. Döbek, Modification of pyrolytic oil from waste tyres as a promising method for light fuel production, Materials (Basel), 2019, 12(6), 880-887. (DOI: 10.3390/ma12060880)
- [29] K. N. Ghimire, K. Inoue, H. Yamaguchi, K. Makino and T. Miyajima, Adsorptive separation of arsenate and arsenite anions from aqueous medium by using orange waste, Water Research, 2003, 37(20), 4945-4953. (DOI: 10.1016/j.watres.2003.08.029)
- [30] J. Shah, M. R. Jan, F. Mabood and M. Shahid, Conversion of waste tires into carbon black and their utilization as adsorbent, Journal of Chinese Chemical Society TAIP, 2006, 53, 1085-1089. (DOI: <https://doi.org/10.1002/jccs.200600144>)
- [31] N. Yalchin and V. Sevinc, Studies of the surface area and porosity of activated carbons prepared from rice husks, Carbon, 2000, 38(14), 1943-1995. (DOI: [https://doi.org/10.1016/S0008-6223\(00\)00029-4](https://doi.org/10.1016/S0008-6223(00)00029-4))
- [32] D. P. Mungasavalli, T. Viraraghavan and Y. C. Jin, Biosorption of chromium from aqueous solutions by pretreated *Aspergillus niger*: Batch and column studies, Colloids and Surfaces A: Physicochemical and Engineering Aspects, 2007, 301(1), 214-223. (DOI: <https://doi.org/10.1016/j.colsurfa.2006.12.060>)
- [33] N V. Chukanov and A. D. Chervonnyi, Infrared Spectroscopy of Minerals and Related Compounds, Springer International Publishing, Switzerland, 2016. (DOI: 10.1007/978-3-319-25349-7_1)

- [34] I. A. Oxtan, O. Knop and M. Falk, Determination of the symmetry of the ammonium ion in crystals from the infrared spectra of the isotopically dilute ammonium-d₁(1+) species. *Journal of Physical Chemistry*, 1976, 80(11), 1212–1217. (DOI: <https://doi.org/10.1021/j100552a019>)
- [35] D. Wu, B. Zhang, C. Li, Z. Zhang and H. Kong, Simultaneous removal of ammonium and phosphate by zeolite synthesized from fly ash as influenced by salt treatment, *Journal of Colloid and Interface Science*, 2006, 304(2), 300-306. (DOI: <https://doi.org/10.1016/j.jcis.2006.09.011>)
- [36] Y. Zheng, Y. Xie and A. Wang, Rapid and wide pH-independent ammonium-nitrogen removal using a composite hydrogel with three-dimensional networks, *Chemical Engineering Journal*, 2012, 179(1), 90-98. (DOI: <https://doi.org/10.1016/j.cej.2011.10.064>)
- [37] H. Liu, Y. Dong, H. Wang and Y. Liu, Adsorption behavior of ammonium by a bio-adsorbent – Boston ivy leaf powder, *Journal of Environmental Sciences*, 2010, 22(10): 1513-1518. (DOI: [https://doi.org/10.1016/S1001-0742\(09\)60282-5](https://doi.org/10.1016/S1001-0742(09)60282-5))
- [38] R. Boopathy, S. Karthikeyan, A. B. Mandal and G. Sekaran. Adsorption of ammonium ion by coconut shell-activated carbon from aqueous solution: Kinetic, isotherm and thermodynamic studies, *Journal of Environmental Science and Pollution Research*, 2013, 20, 533-542. (DOI: [10.1007/s11356-012-0911-3](https://doi.org/10.1007/s11356-012-0911-3))
- [39] A. M. Yusof, L. K. Keat, Z. Ibrahim, Z. A. Majid and N. A. Nizam, Kinetic and equilibrium studies of the removal of ammonium ions from aqueous solution by rice husk ash-synthesized zeolite Y and powdered and granulated forms of mordenite, *Journal of Hazardous Materials*, 2010, 174(1), 380-385. (DOI: [10.1016/j.jhazmat.2009.09.063](https://doi.org/10.1016/j.jhazmat.2009.09.063))
- [40] M. Sarioglu, Removal of ammonium from municipal wastewater using natural Turkish zeolite, *Separation and Purification Technology*, 2005, 41, 1-11. (DOI: <https://doi.org/10.1016/j.seppur.2004.03.008>)